

Bimodal occurrence of aspartoacylase in myelin and cytosol of brain

Jianfeng Wang,* Reuben Matalon,† Gita Bhatia,† Gusheng Wu,* Hong Li,‡ Tong Liu,‡ Zi-Hua Lu* and Robert W. Ledeen*

*Department of Neurology and Neurosciences, New Jersey Medical School, UMDNJ, Newark, New Jersey, USA

†Department of Pediatrics, University of Texas Medical Branch, Children's Hospital, Galveston, Texas, USA

‡Department of Biochemistry and Molecular Biology, New Jersey Medical School, UMDNJ, Newark, New Jersey, USA

Abstract

The growing use of *N*-acetylaspartate as an indicator of neuronal viability has fostered interest in the biological function(s) of this unusual amino acid derivative. In considering the various physiological roles that have been proposed for this relatively abundant molecule one is obliged to take into account its unusual metabolic compartmentalization, according to which synthesis and storage occur in the neuron and hydrolytic cleavage in the oligodendrocyte. The latter reaction, catalyzed by aspartoacylase (ASP), produces acetyl groups plus aspartate and has been proposed to occur in both soluble and membranous subfractions of white matter. Our study supports such bimodal occurrence and we now present

immunoblot, proteomic, and biochemical evidence that the membrane-bound form of ASPA is intrinsic to purified myelin membranes. This was supported by a novel TLC-based method for the assay of ASPA. That observation, together with previous demonstrations of numerous lipid-synthesizing enzymes in myelin, suggests utilization of acetyl groups liberated by myelin-localized ASPA for lipid synthesis within the myelin sheath. Such synthesis might be selective and could explain the deficit of myelin lipids in animals lacking ASPA.

Keywords: aspartoacylase, axon–myelin interaction, myelin, myelin-localized enzymes, myelin lipid synthesis, *N*-acetylaspartate, *N*-acetylaspartate assay.

J. Neurochem. (2007) **101**, 448–457.

N-acetylaspartate (NAA) was revealed as a major amino acid derivative in mammalian brain half a century ago (Tallan *et al.* 1956) and was subsequently shown to be present at high concentrations in most regions of the CNS (Tallan 1957; Marcucci *et al.* 1966). During CNS development, NAA is found in both neurons and oligodendrocytes (OLs) but becomes localized in neurons at maturity (Simmons *et al.* 1991; Urenjak *et al.* 1992; Moffett and Namboodiri 1995). It has thus acquired considerable clinical use in the form of magnetic resonance spectroscopy as a non-invasive indicator of neuronal/axonal viability, several neurological disorders showing depleted NAA (Tsai and Coyle 1995; Clark 1998). Despite this growing clinical utility, the biological function of NAA has remained elusive. The enigma is compounded by its unusual metabolic compartmentalization, synthesis occurring in the neuron (Patel and Clark 1979; Truckenmiller *et al.* 1985) and hydrolytic cleavage of the acetyl group in white matter (D'Adamo *et al.* 1973; Kaul *et al.* 1991). The latter process is catalyzed by *N*-acetyl-L-aspartate amidohydrolase (aspartoacylase, ASPA), reportedly confined to

OLs among cultured rat macroglial cells (Baslow *et al.* 1999). A similar conclusion was reached by *in situ* hybridization histochemistry (Kirmani *et al.* 2002). A vital role for this enzyme in NAA function was suggested by several studies indicating incorporation of NAA-acetyl into brain lipids (D'Adamo and Yatsu 1966; D'Adamo *et al.* 1968; Burri *et al.* 1991; Mehta and Namboodiri 1995). Whereas those studies employed extracellular application of NAA in the form of intracerebral injection or tissue slice

Received April 12, 2006; revised manuscript received October 11, 2006; accepted October 12, 2006.

Address correspondence and reprint requests to Robert W. Ledeen, Department of Neurology and Neurosciences, New Jersey Medical School, UMDNJ, MSB-H506, 185 S. Orange Avenue, Newark, NJ 07103, USA. E-mail: ledeenro@umdnj.edu

Abbreviations used: Ab, antibody; Asp, aspartate; ASPA, Aspartoacylase; BSA, bovine serum albumin; Cyt, cytosol; IgG, immunoglobulin G; MS, mass spectrometry; My, myelin; NAA, *N*-Acetylaspartate; OL, oligodendrocyte; PBS, phosphate-buffered saline; SDS-PAGE, sodium dodecyl sulfate – polyacrylamide gel electrophoresis.

incubation, a subsequent report (Chakraborty *et al.* 2001) demonstrated NAA-acetyl incorporation into myelin (My) lipids from neuronal/axonal localized NAA. This suggested axon–myelin transfer of NAA and hydrolysis within the membrane by myelin-localized ASPA; the latter was demonstrated in that report by biochemical assay of purified rat brain myelin. This was consistent with earlier reports suggesting a membrane/myelin locus for ASPA (Johnson *et al.* 1989; Kaul *et al.* 1991), but was at variance with recent reports that detected ASPA in the soluble fraction but not in myelin. (Klugmann *et al.* 2003; Madhavarao *et al.* 2004). The present study was undertaken to resolve this discrepancy, employing the combined approach of immunoblot, biochemical, and proteomic analyses.

Materials and methods

Myelin isolation

Brains from young adult (~3 months of age) C57BL/6 mice were employed for myelin isolation, either as fresh tissue or after freezing at -80°C for variable periods. The fresh or thawed brain tissue was homogenized in 0.32 mol/L sucrose containing 20 mmol/L Tris–HCl buffer (pH 8.0) and centrifuged at 1500 *g* for 10 min to remove nuclei and cell debris. The supernatant was further centrifuged at 18 000 *g* for 30 min, and the resulting pellet was subjected to myelin purification as previously described (Chakraborty *et al.* 2001). That procedure utilizes three sucrose density gradients, the third of which was a ‘floating up’ gradient to reduce contaminants to a very low level (Haley *et al.* 1981). Supernatant from the 18 000 *g* centrifugation was recentrifuged at 105 000 *g* for 60 min to pellet membranes and produce a cytosolic supernatant. Protease inhibitor cocktail (Sigma, St Louis, MO, USA; Roche, Mannheim, Germany) was present in all operations, which were carried out in the cold. Protein was assayed by the method of Lees and Paxman (1972).

Aspartoacylase antibody preparation

Recombinant mouse ASPA was used as antigen. The plasmid expressing ASPA was in BL21 (DE3) cells of *Escherichia coli* strain purchased from Invitrogen (Carlsbad, CA, USA); the manufacturer’s protocol was used. The expressed protein containing 6×His affinity tag was purified by Ni-nitrilotriacetic acid agarose matrix and the bound protein was eluted using imidazole. The enzyme was further purified using an 8-hydroxyquinoline column. The enzyme preparation with 90–95% purity was used for immunization (Surendran *et al.* 2005). Rabbit polyclonal antibodies (Abs) of immunoglobulin G (IgG) isotype were generated by BioSynthesis Inc. (Lewisville, TX, USA).

Immunoblot analysis and immunoprecipitation

Protein separation was achieved by the method of Laemmli (1970), employing sodium dodecyl sulfate – polyacrylamide gel electrophoresis (SDS–PAGE) with 11% polyacrylamide gel. Myelin samples were dispersed in Laemmli buffer containing 2× the usual SDS concentration. Separated proteins were electrophoretically transferred to a polyvinylidene difluoride membrane and the latter treated with 5.0% bovine serum albumin

(BSA) for 1 h at 25°C . This was followed by ASPA polyclonal Ab, diluted 1 : 500 in phosphate-buffered saline (PBS) containing 2.0% BSA, with exposure overnight at 4°C or 1 h at 25°C . After extensive washing with PBS–0.05% Tween 20 (v/v) (Fisher, Fair Lawn, NJ, USA), incubation was carried out with goat anti-mouse IgG linked to horseradish peroxidase at 25°C for 1 h. Blots were developed on Denville Blue Bio film with ECL reagent (Amersham Biosciences, Piscataway, NJ, USA). As standards we employed ECL DualVue western blotting markers RPN810 (Amersham Biosciences).

For immunoprecipitation, myelin was dispersed in 2.0% Triton X-100 (Sigma) in PBS (pH 7.4) with protease inhibitor cocktail. This was gently agitated at 4°C for 2 h followed by brief centrifugation and protein content determination of the supernatant. Aliquots with ~200 μg protein were pre-absorbed by adding suspension of agarose beads (Sephacrose[®] CL-4B; Sigma) in PBS to total volume of 200 μL and gently shaking at 4°C for 1 h. After brief centrifugation, the resulting supernatant was incubated overnight at 4°C with 20 μL ASPA Ab (IgG, stock diluted 1 : 10) followed by 2 h incubation and gentle shaking with 30 μL Protein G-agarose 4B (Sigma). The beads were pelleted at 3000 *g* for 2 min at 4°C , washed three times with PBS–0.5% Triton X-100 and suspended in 60 μL Laemmli sample buffer; this was boiled for 5 min and centrifuged briefly. Twenty microliters of the supernatant were subjected to SDS–PAGE followed by immunoblot analysis as above.

In-gel digestion and mass spectrometry

Following immunoprecipitation and SDS–PAGE as above, the polyacrylamide gel was stained with GelCode[®] Blue Stain Reagent (Pierce, Rockford, IL, USA) according to manufacturer’s instructions. In addition to the prominent IgG bands, a clearly visible band at ~35 kDa was excised and washed with acetonitrile/water (3 : 7) containing 50 mmol/L ammonium bicarbonate. The gel samples were given to the UMDNJ Center for Advanced Proteomics Research (<http://www.umdnj.edu/proweb>), which carried out trypsin digestion for 2 h on a robotic platform (TECAN, Durham, NC, USA). The resulting peptides were extracted with 30 μL of 1.0% trifluoroacetic acid and mixed with α -cyano-4-hydroxy-cinnamic acid matrix in a 1 : 1 ratio. The mixture was spotted onto a matrix-assisted laser desorption/ionization plate and the peptides analyzed on a 4700 Proteomics Analyzer tandem mass spectrometer (Applied Biosystem, Framingham, MA, USA). Mass spectra (*m/z* 800–3600) were acquired in positive ion reflector mode with internal mass calibration. The 10 most intense ions were selected for subsequent MS/MS sequencing analysis in 1 kV mode. Protein identification was performed by searching the combined MS and MS/MS spectra against all mouse sequences annotated in the SwissProt database (V46) using a local MASCOT search engine (V1.9) on a GPS (V3.5, ABI) server. The following parameters were used: a maximum of one missed cleavage was allowed; precursor mass tolerance was set at 50 ppm and MS/MS mass tolerance at 0.3 Da.

Assay of aspartoacylase

The reaction medium (100 μL) contained 50 mmol/L Tris–HCl (pH 8.5), 50 mmol/L NaCl, 1.0 mmol/L CaCl_2 , 0.1 mmol/L dithiothreitol, 0.5% IGEPAL CA-630 (Sigma; previously termed NP-40), 20 mmol/L NAA to which was added 50–150 μg of myelin or

cytosol (Cyt) protein. After shaking at 37°C for variable times (6 h for routine assays), the reaction was stopped by boiling of the mixture for 5 min followed by brief centrifugation at 16 000 *g*. The reaction supernatant was used for quantification of liberated aspartate (Asp). Controls (blanks) were obtained by prior boiling of equivalent samples for 5 min. The presence of detergent (e.g., IGEPAL CA-630) was essential for myelin assay but not for cytosol. Two methods were employed for determining liberated Asp: (i) a previously described enzymatic assay and (ii) a new procedure based on TLC-densitometric determination of free Asp. The first of these, based on the coupled enzyme system of Fleming and Lowry (1966), was similar to that employed by Chakraborty *et al.* (2001) with some modifications. The amount of liberated Asp was quantified by addition of 20 μ L reaction supernatant to a mixture of 25 mmol/L Tris-HCl buffer (pH 8.0), 25 mmol/L NaCl, 1 mmol/L α -ketoglutarate, 75 μ mol/L NADH, 0.5 mg/mL BSA, 1 U of Asp aminotransferase and 5 U of malate dehydrogenase in a total volume of 1 mL. After 1 h incubation at 37°C, the mixture was centrifuged at 16 000 *g* for 5 min and the optical density of the supernatant at 340 nm was determined. Decrease in absorbance at 340 nm indicated conversion of NADH to NAD⁺ in the coupled reaction. A standard curve was created by assaying variable amounts (2.5–25 μ g) of Asp. Background blanks for these assays and those based on TLC (see below) were determined by preparing the complete mixture, including NAA and tissue, and immediately boiling for 5 min.

For TLC-densitometry, 10 μ L of reaction supernatant was applied to a glass-backed 10 \times 20 cm TLC plate (silica gel 60), along with varying amounts of standard Asp. The plate was developed in ethyl acetate/methanol/formic acid/water (60/30/6/5, by vol.). After drying, the plate was sprayed with 1.0% (w/v) ninhydrin in 1-butanol/acetic acid (95/5, v/v), placed in the hood until dry, covered with a glass plate and heated in a 110°C oven until Asp bands became visible (\sim 3 min). This amount of heating gave well-defined reddish-purple bands with relatively little background, whereas over-heating converted the bands to brownish color and gave interfering background. Soon after cooling, the plate was scanned with an HP Scanjet 7450 flat scanner (Hewlett Packard, Palo Alto, CA, USA) and the density of Asp bands determined with a FluoChemTM digital imaging system (Alphainnotech.com). Quantification was achieved with a standard curve obtained with Asp standards on the same TLC plate. NAA, which was well separated on the plate from Asp, was not revealed by this procedure.

Properties of aspartoacylase

Enzymatic properties of ASPA in myelin and cytosol were determined by the above coupled reaction procedure and in some cases by the TLC method as well. Kinetic parameters were estimated by employing a range (0.25–40 mmol/L) of NAA concentrations and generating a Lineweaver–Burk plot by GraphPad Prism V4.02 (GraphPad Inc, San Diego, CA, USA). This revealed an optimal concentration of NAA as \sim 20 mmol/L, which was used in subsequent experiments to determine pH optima and variation of activity with time and protein. To test for intrinsic versus loosely associated enzyme, myelin samples were dispersed in 20 mmol/L Tris-HCl (pH 8.0) buffer with added NaCl (0.5 mol/L) or sodium taurocholate (0.1%) and stirred for 45 min at 0°C (Chakraborty

et al. 2001). After pelleting and washing with PBS, the resulting myelin was assayed in the above reaction medium as described.

Results

Immunoblot analysis

Immunoblot analysis of fractions from normal mouse brain, utilizing polyclonal Ab to ASPA, revealed a strong band for both myelin and cytosol at \sim 35 kDa apparent molecular weight (Fig. 1a). This corresponded to the predicted molecular mass of 35.3 kDa for mouse ASPA (Matalon *et al.* 2000). Some additional less prominent bands were observed, especially in the cytosol pattern. The band at \sim 28 kDa is considered a possible degradation product of the holoprotein, because it increased when less protease inhibitor was used during myelin isolation, whereas the band at \sim 70–75 kDa might correspond to an ASPA dimer, in keeping with the presumed dimer observed in rat brain extract (Klugmann *et al.* 2003) and the murine ASPA expressed by *E. coli* (Moore *et al.* 2003). It is important to note that the gel depicted in Fig. 1a was obtained from fractions isolated from relatively fresh brain: \sim 1 h freezing at -80°C . Freezing of the brain at -80°C for 2 days prior to subfraction isolation resulted in modest decrease of the 35 kDa band in myelin (Fig. 1b, My-2), when compared with myelin obtained from fresh brain (Fig. 1b, My-1). Brain frozen for 1 year gave myelin that showed virtually none of the 35 kDa band (Fig. 1b, My-3). In contrast, cytosol from those same brains showed corresponding increases in the 35 kDa band, especially noticeable for the 1-year frozen brain (Fig. 1b, Cyt-3). This suggests that prolonged freezing somehow disrupts the ASPA-myelin association, causing appearance of this ASPA in the cytosol fraction.

Immunoprecipitation and mass spectrometric analysis

To confirm identity of the above 35 kDa band, immunoprecipitation of myelin was carried out with rabbit polyclonal Ab to the ASPA protein and the precipitated protein subjected to SDS-PAGE as described above (Fig. 1c). The 35 kDa band was excised, subjected to mass spectrometric analysis, and protein identification was achieved by searching the combined MS and MS/MS spectra against the SwissProt database (V46) using a local MASCOT search engine (V1.9) on a GPS (V3.5, ABI) server. Based on MS spectrum, seven peptides (one an oxidized form) were matched to mouse ASPA II (312aa, 35.3 kDa) with the sequence coverage of 19.0%. Two peptide sequences, AGLDVKPFITNPR and AQEINHFLFGPK were further confirmed by MS/MS sequencing analysis (nos 2 and 6, Table 1). The protein score confidence interval value was 99.97%. The 35 kDa protein obtained from purified myelin is thus in accord with the amino acid sequence previously reported for ASPA (Kaul *et al.* 1993), shown in Table 1.

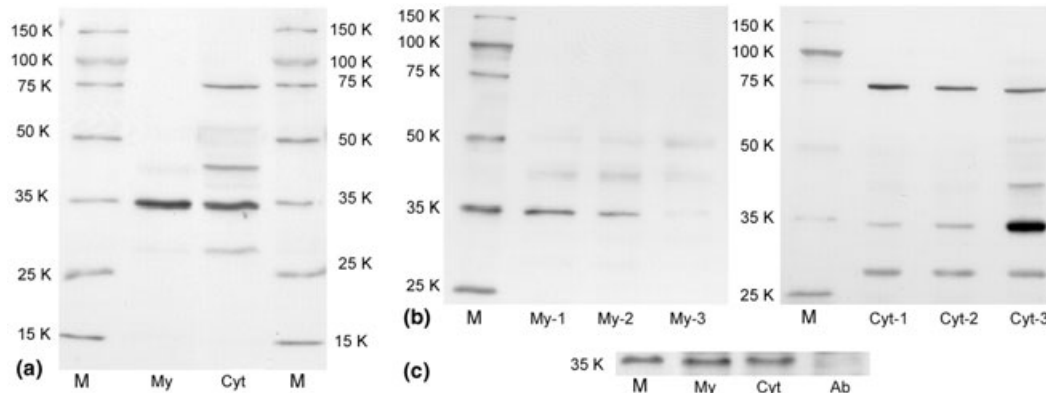


Fig. 1 Western blot detection of ASPA in myelin and cytosol of mouse brain. (a) SDS-PAGE (11% acrylamide) was carried out with purified myelin (My) (26 μ g protein) and cytosol (Cyt) (15 μ g protein) from C57BL/6 mouse brains, followed by electrophoretic transfer to PVDF membrane. Blotting was performed with rabbit polyclonal Ab to recombinant mouse ASPA, followed by goat anti-mouse IgG linked to HRP. One clear band was visible for My at \sim 35 kDa, corresponding to the molecular weight for mouse ASPA. Cyt showed the same major band at 35 kDa and a few additional less prominent bands. (b) Comparison of My and Cyt from mouse brains after variable periods of storage at -80°C . My-1 and Cyt-1 from fresh brain; My-2 and Cyt-2 from brain frozen for 2 days; My-3 and Cyt-3 from brain frozen for

1 year. Western blot performed as in (a). Two days storage at -80°C produced a moderate decrease in the 35 kDa ASPA band of myelin (My-2) while 1 year of frozen storage virtually eliminated that band from myelin (My-3). There was a corresponding increase in the 35 kDa band of cytosol (Cyt-3). (c) Immunoprecipitation of ASPA. Purified mouse myelin was solubilized and immunoprecipitated with the above Ab as described. Shown is SDS-PAGE of the resulting precipitate followed by western blot, showing the expected ASPA band at 35 kDa. This was well separated from the immunoglobulin bands (not shown). For proteomic analysis, a similar gel was run and stained with Gel-Code[®] Blue Stain Reagent followed by excision of the band and MS/MS analysis (see Materials and methods section and Table 1).

Table 1 Aspartoacylase identification in myelin with mass spectrometric analysis

A	Observed [M+H] ⁺	Calculated [M+H] ⁺	Delta	Sequence	Start-end
1	1064.5623	1064.6085	0.0462	R.VFDLENLSK.E	71-79
2	1253.6637	1253.6801	0.0164	R.AQEINHFLGPK.N*	92-102
3	1367.6147	1367.6483	0.0336	K.EMSEDLPEYEV.R	80-90
4	1383.6096	1384.6473	0.0377	K.EMSEDLPEYEV.R Oxidation (M)	80-90
5	1409.7648	1409.7573	-0.0075	R.RAQEINHFLGPK.N	91-102
6	1427.8005	1427.8025	0.0020	R.AGLDVKPFITNPR.A*	43-55
7	1717.9384	1717.9382	-0.0002	K.YPVGIEVGPQPHGVLR.A	172-187
B	Rank protein name		Accession no.	Protein score (CI%)	
	Aspartoacylase (aminoacylase) II (<i>Mus musculus</i>)		gil19354304	99.966	
C	Protein sequence				
1	MTSCVAKEPIKIIAIFGGTHGNELTGVFLVTHWLRNGTEVHRAGLDVKKPF				
51	ITNPRAVEKCTRYIDCDLNRVFDLENLSKEMSEDLPEYEVRRAQEINHFLG				
101	PKNSDDAYDIVFDLHNTTSNMGCTLILEDNRDFLIQMFHYIKTCMAPLP				
151	CSVYLIEHPSLKYATTRSIAK YPVGIEVGPQPHGVLR ADILDQMRKMIKH				
201	ALDFIQHFNEGKEFPFPCSIDVYKIMEKVDYPRNESGDMAAVIHPNLQDQD				
251	WKPLHPGDPVVFVSLDGVKVIPLGGDCTVYPVFNAAAYYEKKEAFKTKL				
301	TLSAKSIRSTLH				

Sample immunoprecipitated with anti-ASPA was subjected to SDS-PAGE and \sim 35 kDa band was trypsin-digested. Proteomic analysis revealed seven most prominent peptides (A), two of them (marked with * in A) being further analyzed by MS/MS. The identified peptides matched to mice aspartoacylase II at high score (B) with 19% coverage (bold letters in C) of whole sequence of the aspartoacylase.

New assay method for aspartoacylase

To further characterize myelin-localized ASPA, we developed an improved method for assaying this enzyme based on

TLC-densitometry. Asp liberated from NAA by ASPA was separated from NAA by TLC employing ethyl acetate/methanol/formic acid/water (60/30/6/5, by vol.) as solvent.

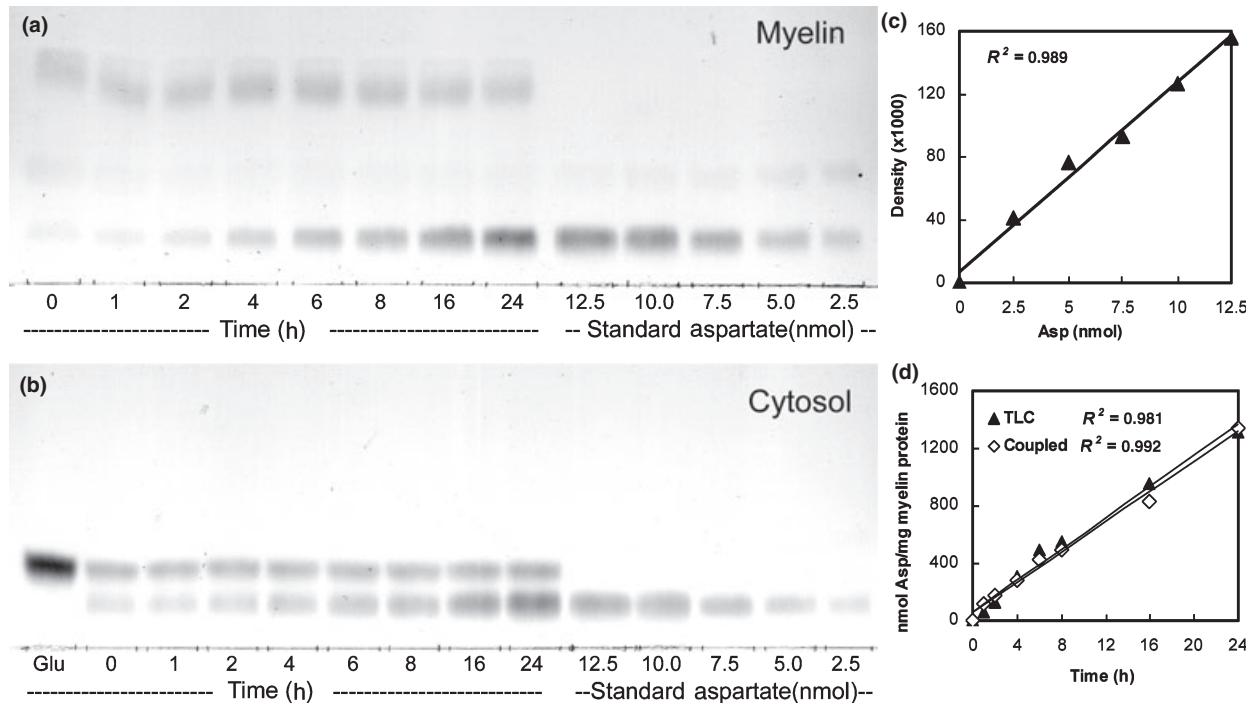


Fig. 2 Assay of ASPA by TLC detection of liberated Asp. Following reaction of myelin or cytosol with NAA and brief centrifugation, supernatant was applied to TLC plate (silica gel G), which was developed in ethyl acetate/methanol/formic acid/water (60/30/6/5 by vol.). After drying, the plate was sprayed with 1% ninhydrin and bands visualized by heating as described. Analysis of myelin (a: 76 μ g protein/sample) revealed Asp to increase with time. Upper band is Triton

X-100. Analysis of cytosol (b: 106 μ g protein/sample) revealed Asp in addition to glutamate running just ahead of, but well separated from Asp. Standards of Asp run on the same plate were used for densitometric quantification. Validity of the TLC method was shown in the linearity of the densitometric response to variable Asp amounts (c). Comparison of the TLC method with the coupled enzyme reaction showed virtually identical results for the two methods (d).

Free Asp was visualized by ninhydrin spray and brief heating at 110°C. Time-dependent changes in ASPA-liberated Asp were seen on TLC for both myelin (Fig. 2a) and cytosol (Fig. 2b). Glutamate, if present (e.g., in cytosol), was also revealed but was well separated from Asp (Fig. 2b). Densitometric analysis showed linearity of response to Asp standards (Fig. 2c). Moreover, quantification by this method appeared identical to that achieved by the coupled reaction system previously employed (Fig. 2d; Chakraborty *et al.* 2001). This TLC procedure, which requires no radiolabeled substrate, differs from that previously described, which utilizes radiolabeled NAA and phosphor imaging of the [14 C]Asp product (Madhavarao *et al.* 2002, 2004). The importance of detergent in assay of myelin ASPA was noted (see above); no activity was detected in its absence. Our previous study (Chakraborty *et al.* 2001) employed relatively low concentration (0.05%) of NP-40 (IGEPAL CA-630), which may account for the observed 1-h delay in release of ASPA activity from myelin in that study. In the present study, use of higher concentration (0.5% IGEPAL CA-630) resulted in no delay and also improved myelin dispersion. As expected, detergent had little effect in the assay of cytosol.

Enzymatic properties of myelin aspartoacylase

Kinetic parameters of myelin and cytosol ASPA were determined by variation of substrate concentration and generation of Lineweaver–Burk plots (Fig. 3a). V_{\max} -values for ASPA of myelin and cytosol (102 and 88.4 nmol/mg protein/h, respectively) were similar, whereas the K_m -values (3.75 and 1.69 mmol/L for myelin and cytosol, respectively) were significantly different. The optimal concentration of NAA was approximately 20 mmol/L, which was used in subsequent experiments. Determination of pH optima revealed values \sim 8.0–8.5 for both myelin and cytosol, although there were observable differences between the curves at lower and higher pH (Fig. 3b). Linearity with respect to time was observed for both myelin and cytosol ASPA, such linearity extending to at least 24 h (Fig. 3c). On that basis, we adopted 6 h as standard reaction time for most experiments. Linearity was also observed with respect to protein in the range 25–150 μ g (Fig. 3d).

To determine whether the myelin enzyme is truly intrinsic to this membrane, samples of the latter were agitated with 0.1% sodium taurocholate or 0.5 mol/L NaCl at 0°C for 45 min prior to ASPA assay. Using these standard methods for removal of loosely associated proteins, myelin activity

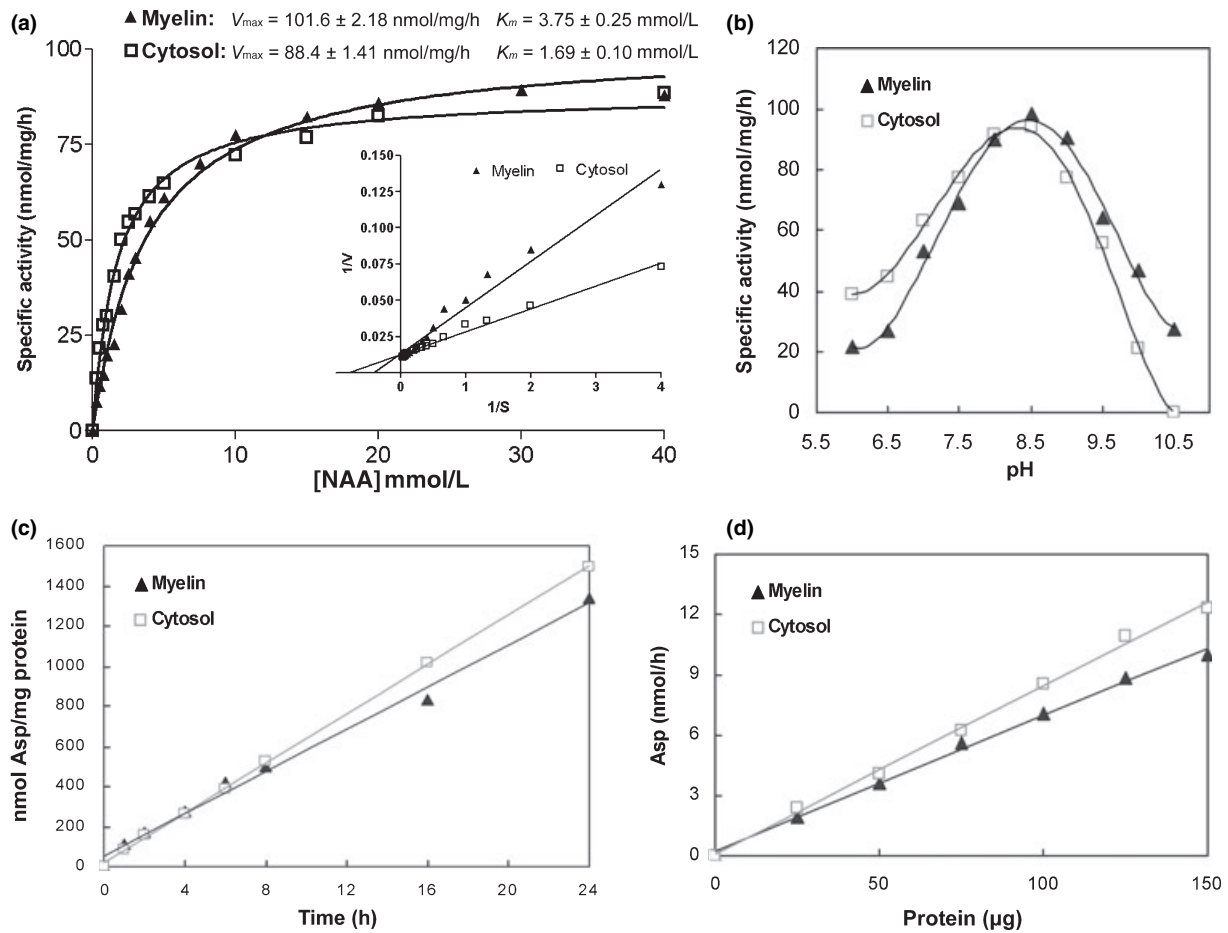


Fig. 3 Determination of enzyme kinetics and properties. (a) Aspartoacylase activities in myelin and cytosol were determined as function of NAA concentration. Lineweaver–Burk plot provided V_{max} and K_m values. (b) Variation of ASPA activity with pH. Myelin and cytosol both

showed pH optimum in the range 8.0–8.5. However, differences were seen in the curves at lower and higher pH. (c) ASPA activity for both myelin and cytosol was linear with respect to time up to 24 h. (d) The assay was also linear with respect to protein in the range shown.

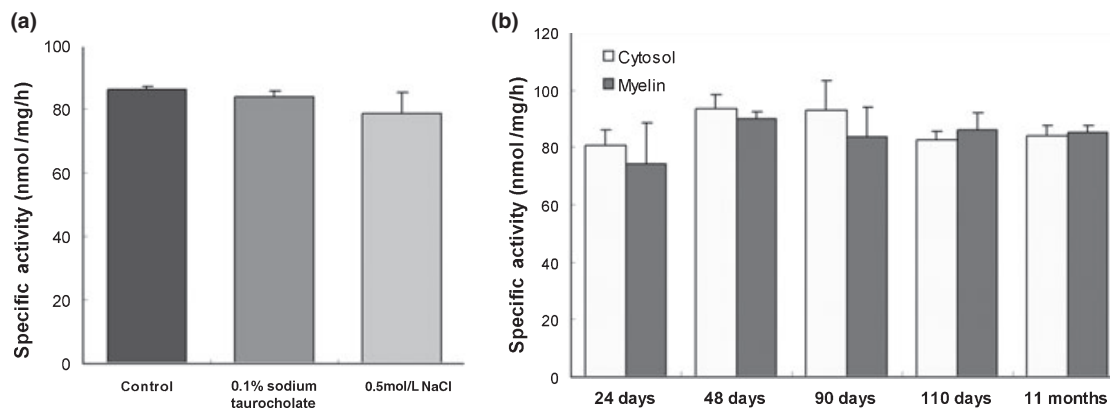


Fig. 4 (a) Test for myelin-intrinsic activity. Samples of purified myelin (93 μ g protein/sample) were agitated in the cold for 30 min with 0.1% Na-taurocholate or 0.5 mol/L NaCl, followed by centrifugation and assay. Specific activity of ASPA was not significantly decreased by

either treatment, designed to remove loosely associated proteins. (b) Assay of myelin and cytosol in mice of different ages showed no decrease in ASPA activity with maturation/aging.

was found to decrease only 2.3% and 8.7%, respectively, after these treatments (Fig. 4a). This indicated ASPA to be an integral component of the myelin sheath and not adventitiously adsorbed during isolation.

Aspartoacylase activity as function of age

The ASPA activities in myelin isolated from mice of variable age were compared (Fig. 4b). Except for 24-day-old mice, whose myelin ASPA activity (74.3 ± 14 nmol/mg/h) was slightly lower, all myelin samples showed similar activity in the range 80–90 nmol/mg/h. In that regard, ASPA differs from certain other myelin enzymes that show significant decline with maturation/aging (Cf., Ledeen 1992).

Discussion

Early studies on the biological function of NAA by D'Adamo *et al.* showed the acetyl group of this molecule to be incorporated into rat brain lipids (D'Adamo and Yatsu 1966; D'Adamo *et al.* 1968). Burri *et al.* (1991) extended that concept in showing NAA to be a major source of acetyl groups for lipid synthesis during brain development with more efficient incorporation than free acetate. Along similar lines, Mehta and Nambodiri (1995) proposed that NAA serves as a storage form of acetate for acetyl-CoA formation. Those studies and conclusions were largely based on experiments in which NAA was applied via extracellular mode in the form of brain injection or tissue incubation. Another approach, which took into account that NAA occurs mainly as an intraneuronal store, utilized the rat optic system to show that neuronal/axonal-localized NAA containing radiolabeled acetyl contributed the latter group to adjacent myelin for lipid synthesis (Chakraborty *et al.* 2001). The evidence suggested that this resulted from NAA behaving like certain other lipid precursors in undergoing axon-to-myelin transfer followed by incorporation into lipid(s) via myelin-localized enzymes (for review: Ledeen 1992).

N-Acetylaspartate functioning in this manner suggested the possible presence of ASPA in the myelin membrane, and evidence for this was initially presented in the form of biochemical assay of isolated myelin (Chakraborty *et al.* 2001). However, subsequent studies in other labs reported biochemical detection of ASPA in cytosol but not in myelin (Klugmann *et al.* 2003; Madhavarao *et al.* 2004). Moreover, the latter studies employing immunocytochemistry detected ASPA in OL cell bodies but not myelin *per se*, and also failed to detect ASPA in myelin by western blot analysis. The reason for this discrepancy is not clear, but may derive from methodological differences (see below). In the present study, we have re-examined myelin more rigorously by a combination of western blot, proteomic, and biochemical analyses. Using an Ab raised to recombinant ASPA, a single band of correct molecular weight (~35 kDa) was detected (Fig. 1), and MS proteomic analysis of this material following

immunoprecipitation showed ASPA as the major component. In this study, we noted that the 35-kDa band in myelin was quite prominent when western blot analysis was carried out with myelin isolated from relatively fresh brain, in contrast to myelin from frozen brain which gave a band of significantly reduced intensity (Fig. 1b). This proved to be time dependent in that myelin from brain that had been frozen 2 days showed modest reduction (Fig. 1b, My-2), whereas myelin from brain that was frozen 1 year showed virtually no ASPA by western blot analysis (Fig. 1b, My-3). In contrast, the amount of ASPA detected in cytosol from the latter brain rose significantly (Fig. 1b, Cyt-3), suggesting acquisition from the myelin locus. Prolonged freezing, possibly in combination with subsequent thawing, apparently disrupted the association of ASPA with myelin by an as-yet-undetermined mechanism. Similar shifts in subcellular distribution have been reported for other membrane proteins following prolonged freezing of brain (Stahl and Swanson 1975) and other tissue (Tochigi *et al.* 1986). However, it may be noted that the association of ASPA with myelin from unfrozen brain proved strong enough to survive treatment with 0.5 mol/L NaCl and 0.1% Na-taurocholate (Fig. 4a), agents that normally remove loosely associated proteins from membranes. The above reports that found little or no western blot evidence for ASPA in myelin did not indicate the history of the brains used as myelin source.

In addition to such considerations, another important factor in regard to ASPA detection is use of adequate detergent to release ASPA from its myelin association. Although ASPA was initially described as a soluble enzyme (D'Adamo *et al.* 1973, 1977), it was also characterized as membrane-bound (Goldstein 1976) and Kaul *et al.* (1991) pointed to the requirement of detergent for solubilization of the enzyme as evidence of membrane association. Our experience has reinforced the latter observation: earlier use of only 0.05% NP-40/IGEPAL CA-630 likely accounted for the 1–2 h delay we observed in reaction onset (Chakraborty *et al.* 2001), in contrast to the present study employing 0.5% of the same detergent in which no delay was observed (Fig. 3c). In contrast to cytosol, which required no detergent, no liberated Asp could be detected in myelin in the absence of detergent. The above-mentioned report (Madhavarao *et al.* 2004) in which biochemical analysis failed to detect ASPA in myelin employed 0.05% IGEPAL CA-630 for a limited period (1 h at 37°C). The other negative report (Klugmann *et al.* 2003) failed to give experimental details on that point. The same principle may apply to western blot analysis, and the fact that we solubilized myelin in Laemmli buffer containing twice the usual SDS concentration for SDS-PAGE likely accounted for the facile detection of ASPA (Fig. 1). The difficulty in immunohistochemical detection may similarly represent a crypticity phenomenon resulting from sequestration of ASPA within the lipid-rich myelin sheath.

In contrast to myelin, which showed primarily one band at ~35 kDa, western blot analysis of cytosol showed three additional bands. The one at ~70–75 kDa is presumably the previously reported dimer (Klugmann *et al.* 2003; Moore *et al.* 2003) and the ~28 kDa protein is possibly a degradation product of 35 kDa ASPA. The band at ~45 kDa is of unknown identity. Identification of soluble and membrane compartments as the loci of ASPA likely refers to subfractions of the OL, the primary cell type in which ASPA is localized (Baslow *et al.* 1999; Bhakoo *et al.* 2001; Klugmann *et al.* 2003; Madhavarao *et al.* 2004). In considering the relative amounts of ASPA in these two subcompartments, our previous study of brainstem indicated the total content in myelin to approximate half that of cytosol (Chakraborty *et al.* 2001). However, our present results indicate that such apportionment is variable and dependent on the history of the brain tissue prior to myelin isolation. In reporting bimodal occurrence of ASPA in myelin and cytosol, we do not preclude its possible presence in other subcellular fractions, especially in view of the reported bimodal occurrence of NAA-synthase in both microsomes and mitochondria (Lu *et al.* 2004).

In demonstrating ASPA activity in myelin biochemically, we have developed a new assay based on TLC separation and ninhydrin visualization of liberated Asp (Fig. 2). This gave results comparable to the previously employed coupled reaction system with malate dehydrogenase and Asp aminotransferase (Fleming and Lowry 1966; Chakraborty *et al.* 2001) (Fig. 2d). However, the new method proved more definitive and in some respects more convenient than the latter. Our analyses indicated similar V_{\max} -values for ASPA in myelin and cytosol but a K_m -value for myelin approximately twice that of cytosol (Fig. 4). This difference is possibly because of difference(s) in post-translational processing that is likely required to render a portion of the enzyme membrane-associated. Only slight differences in pH optima were observed (Fig. 3b), although there were apparently significant differences between the curves at lower and higher pH (Fig. 3b). Biochemical analysis following treatment with NaCl and Na-taurocholate was used to demonstrate that myelin-associated ASPA is truly intrinsic to the membrane (Fig. 4a).

The presence of ASPA in myelin provides an interesting addition to the long list of lipid synthesizing and metabolizing enzymes that have been identified as integral components of purified myelin (for review: Norton and Cammer 1984; Ledeen 1992). Of special significance are the recently discovered fatty acid synthesizing enzymes, acetyl-CoA carboxylase and fatty acid synthase (Chakraborty and Ledeen 2003). The latter enzyme complex in purified myelin showed amazingly high activity, approximating half that of its cytosolic counterpart, and it differed from the latter in requiring detergent. These are the enzymes that would utilize ASPA-liberated acetyl groups to form fatty acids, which are

then presumably incorporated into myelin lipids by various enzymes also shown to occur in this membrane. These include the reactions leading to the synthesis of choline- and ethanolamine-phosphoglycerides, the major phospholipids of myelin (for review: Ledeen 1992). NAA can thus be added to the list of precursors shown to undergo axon-to-myelin transfer with subsequent incorporation into myelin lipids, which thus far include choline (Droz *et al.* 1978), phosphate (Ledeen and Haley 1983), acyl chains (Toews and Morell 1981; Alberghina *et al.* 1982), and serine (Haley and Ledeen 1979). The mechanism of this intercellular transfer remains to be elucidated.

Additional evidence for a role of NAA and ASPA in myelinogenesis was recently presented in a study showing significantly more NAA-synthase activity in neurons that extend myelinated axons when compared with those whose axons are unmyelinated (Ledeen *et al.* 2006). In proposing this function for NAA and ASPA, it is necessary to emphasize that this is not viewed by us as the sole or even major pathway for myelin lipid synthesis. Myelination proceeds to a significant degree in the absence of ASPA-generated NAA-derived acetyl groups, as seen, for example, in Canavan disease and its animal models characterized by mutated and hence non-functional ASPA. In these cases, myelination does occur, although the membrane structure is morphologically abnormal (Matalon *et al.* 2000). The parallel pathways within the OL are undoubtedly most prominent during initial myelinogenesis when the OL might be less dependent on the axon for metabolic support, and conceivably the NAA/ASPA pathway could function in relation to myelin maintenance over time when the axon would be expected to have a more active role. This would be consistent with our observation that myelin-localized ASPA retains full activity throughout the first year of the mouse's life (Fig. 4b). Nevertheless, the ASPA-null mouse showed decreased levels of total brain myelin (Ledeen *et al.* 2006) as well as deficits of specific myelin lipids (Madhavarao *et al.* 2005; Ledeen *et al.* 2006).

Yet more evidence for NAA/ASPA participation in CNS myelinogenesis came from the recent study of Jalil *et al.* (2005), showing that Aralar (-/-) mice lacking the mitochondrial Asp-glutamate carrier showed marked reduction of brain NAA along with reduced myelin synthesis. They interpreted this as support for the previous finding that NAA synthesis occurs predominantly in microsomes as opposed to mitochondria (Lu *et al.* 2004). Remaining to be determined are the relative contributions to myelin lipid synthesis at various stages of development/maturation of the intrinsic OL mechanisms versus the NAA/ASPA pathways in myelin and OL cytosol. It will also be of interest to explore how NAA deficits reported in several other neurological disorders (Tsai and Coyle 1995) might affect the chemical composition and fine structure of myelin over time.

Acknowledgements

This work was supported by a grant from Jacob's Cure: A Fight Against Canavan Disease.

References

- Alberghina M. M., Viola M. and Giuffrida A. M. (1982) Transfer of axonally transported phospholipids into myelin isolated from rabbit optic pathway. *Neurochem. Res.* **7**, 139–149.
- Baslow M. H., Suckow R., Saperstein V. and Hungund B. L. (1999) Expression of aspartoacylase activity in cultured rat macro glial cells is limited to oligodendrocytes. *J. Mol. Neurosci.* **13**, 47–53.
- Bhakoo K. K., Craig T. J. and Styles P. (2001) Developmental and regional distribution of aspartoacylase in rat brain tissue. *J. Neurochem.* **79**, 211–220.
- Burri R., Steffen C. and Herschkowitz N. (1991) *N*-Acetyl-L-aspartate is a major source of acetyl groups for lipid synthesis during rat brain development. *Dev. Neurosci.* **13**, 403–411.
- Chakraborty G. and Ledeen R. W. (2003) Fatty acid synthesizing enzymes intrinsic to myelin. *Mol. Brain Res.* **112**, 46–52.
- Chakraborty G., Mekala P., Yahya D., Wu G. and Ledeen R. W. (2001) Intraneuronal *N*-acetylaspartate supplies acetyl groups for myelin lipid synthesis: evidence for myelin-associated aspartoacylase. *J. Neurochem.* **78**, 736–745.
- Clark J. B. (1998) *N*-Acetyl aspartate: a marker for neuronal loss or mitochondrial dysfunction. *Dev. Neurosci.* **20**, 271–276.
- D'Adamo A. F. and Yatsu F. M. (1966) Acetate metabolism in the nervous system. *N*-acetyl-L-aspartic acid and the biosynthesis of brain lipids. *J. Neurochem.* **13**, 961–963.
- D'Adamo A. F., Gidez L. I. and Yatsu F. M. (1968) Acetyl transport mechanisms. Involvement of *N*-acetyl aspartic acid in de novo fatty acid biosynthesis in the developing rat brain. *Exp. Brain Res.* **5**, 267–273.
- D'Adamo A. F., Smith J. C. and Woiler C. (1973) The occurrence of *N*-acetylaspartate amidohydrolase (aminoacylase II) in the developing rat. *J. Neurochem.* **20**, 1275–1278.
- D'Adamo A. F., Peisach J., Manner G. and Weiler C. T. (1977) *N*-Acetyl-aspartate amidohydrolase: purification and properties. *J. Neurochem.* **28**, 739–744.
- Droz B., Di Giamberardino L., Koenig H. L., Boyenval J. and Hassig R. (1978) Axon-myelin transfer of phospholipid components in the course of their axonal-transport as visualized by radioautography. *Brain Res.* **155**, 347–353.
- Fleming M. C. and Lowry O. H. (1966) The measurement of free and *N*-acetylated aspartic acids in the nervous system. *J. Neurochem.* **13**, 779–783.
- Goldstein F. B. (1976) Amidohydrolases of brain: enzymatic hydrolysis of *N*-acetyl-L-aspartate and other *N*-acetyl-L-amino acids. *J. Neurochem.* **26**, 45–49.
- Haley J. E. and Ledeen R. W. (1979) Incorporation of axonally transported substances into myelin lipids. *J. Neurochem.* **32**, 735–742.
- Haley J. E., Samuels F. G. and Ledeen R. W. (1981) Study of myelin purity in relation to axonal contaminants. *Cell. Mol. Neurobiol.* **1**, 175–187.
- Jalil M. A., Begum L., Contreras L. *et al.* (2005) Reduced *N*-acetylaspartate levels in mice lacking aralar, a brain- and muscle-type mitochondrial aspartate-glutamate carrier. *J. Biol. Chem.* **280**, 31 333–31 339.
- Johnson A. B., Kaul R., Casanova J. and Matalon R. (1989) Aspartoacylase, the deficient enzyme in spongy degeneration (Canavan disease) is a myelin-associated enzyme. *J. Neuropathol. Exp. Neurol.* **48**, 349. (Abstract).
- Kaul R., Casanova J., Johnson A. B., Tang P. and Matalon R. (1991) Purification, characterization, and localization of aspartoacylase from bovine brain. *J. Neurochem.* **56**, 129–135.
- Kaul R., Gao G. P., Balamurugan K. and Matalon R. (1993) Human aspartoacylase cDNA and missense mutation in Canavan disease. *Nat. Genet.* **5**, 118–123.
- Kirmanli B. F., Jacobowitz D. M., Kallarakal A. T. and Namboodiri M. A. (2002) Aspartoacylase is restricted primarily to myelin synthesizing cells in the CNS: therapeutic implications for Canavan disease. *Brain Res. Mol. Brain Res.* **107**, 176–182.
- Klugmann M., Symes C. W., Klausner B. K., Leichtlein C. B., Serikawa T., Young D. and Doring M. J. (2003) Identification and distribution of aspartoacylase in the postnatal rat brain. *Neuroreport* **14**, 1837–1840.
- Laemmli U. K. (1970) Cleavage of structural proteins during the assembly of the head of bacteriophage T4. *Nature* **227**, 680–685.
- Ledeen R. W. (1992) Enzymes and receptors of myelin, in *Myelin: Biology and Chemistry* (Martenson R. E., ed.), pp. 527–566. CRC Press, Boca Raton, Florida.
- Ledeen R. W. and Haley J. E. (1983) Axon-myelin transfer of glycerol-labeled lipids and inorganic phosphate during axonal transport. *Brain Res.* **269**, 267–275.
- Ledeen R. W., Wang J., Wu G., Lu Z. H., Chakraborty G., Meyenhofer M., Tying S. K. and Matalon R. (2006) Physiological role of *N*-acetylaspartate: contribution to myelinogenesis, in *N-acetylaspartate: A Unique Neuronal Molecule in the Central Nervous System* (Moffett J. R., Tieman S. B., Weinberger D. R., Coyle J. T. and Namboodiri M. A., eds.), pp. 131–143. Springer Science, New York.
- Lees M. and Paxman S. (1972) Modification of the Lowry procedure for the analysis of proteolipid protein. *Analyt. Biochem.* **47**, 184–192.
- Lu Z.-H., Chakraborty G., Ledeen R. W., Yahya D. and Wu G. (2004) *N*-Acetylaspartate synthase is bimodally expressed in microsomes and mitochondria of brain. *Mol. Brain Res.* **122**, 71–78.
- Madhavarao C. N., Hammer J. A., Quarles R. H. and Namboodiri M. A. (2002) A radiometric assay for aspartoacylase activity in cultured oligodendrocytes. *Anal. Biochem.* **308**, 314–319.
- Madhavarao C. N., Moffett J. R., Moore R. A., Viola R. E., Namboodiri M. A. and Jacobowitz D. M. (2004) Immunohistochemical localization of aspartoacylase in the rat central nervous system. *J. Comp. Neurol.* **472**, 318–329.
- Madhavarao C. N., Arun P., Moffett J. R. *et al.* (2005) Defective *N*-acetylaspartate catabolism reduces brain acetate levels and myelin lipid synthesis in Canavan's disease. *Proc. Natl Acad. Sci. USA* **102**, 5221–5226.
- Marcucci F., Mussini E., Valzelli L. and Garattini S. (1966) Distribution of *N*-acetyl-L-aspartic acid in rat brain. *J. Neurochem.* **13**, 1069–1070.
- Matalon R., Rady P. L., Platt K. A. *et al.* (2000) Knock-out mouse for Canavan disease: a model for gene transfer to the central nervous system. *J. Gene Med.* **2**, 165–175.
- Mehta V. and Namboodiri M. A. (1995) *N*-Acetylaspartate as an acetyl source in the nervous system. *Mol. Brain Res.* **31**, 151–157.
- Moffett J. R. and Namboodiri M. A. (1995) Differential distribution of *N*-acetylaspartate-L-glutamate and *N*-acetylaspartate immunoreactivities in rat brain. *J. Neurocytol.* **24**, 409–433.
- Moore R. A., Le Coq J., Faehnle C. R. and Viola R. E. (2003) Purification and preliminary characterization of brain aspartoacylase. *Arch. Biochem. Biophys.* **413**, 1–8.
- Norton W. T. and Cammer W. (1984) Isolation and characterization of myelin, in *Myelin* (Morell P., ed.), pp. 147–195. Plenum Press, New York.

- Patel T. B. and Clark J. B. (1979) Synthesis of *N*-acetyl-L-aspartate by rat brain mitochondria and its involvement in mitochondrial/cytosolic carbon transport. *Biochem. J.* **184**, 539–546.
- Simmons M. D., Frondoza C. G. and Coyle J. T. (1991) Immunocytochemical localization of *N*-acetylaspartate with monoclonal antibodies. *Neuroscience* **45**, 37–45.
- Stahl W. L. and Swanson P. D. (1975) Effects of freezing and storage on subcellular fractionation of guinea pig and human brain. *Neurobiology* **5**, 393–400.
- Surendran S., Campbell G. A., Tyring S. K. and Matalon R. (2005) Aspartoacylase gene knockout results in severe vacuolation in the white matter and gray matter of the spinal cord in the mouse. *Neurobiol. Dis.* **18**, 385–389.
- Tallan H. H. (1957) Studies on the distribution of *N*-acetyl-L-aspartic acid in brain. *J. Biol. Chem.* **224**, 41–45.
- Tallan H. H., Moore S. and Stein W. H. (1956) *N*-acetyl-L-aspartic acid in brain. *J. Biol. Chem.* **219**, 257–264.
- Tochigi B., Osawa Y. and Osawa Y. (1986) The apparent shift in distribution of aromatase activity in the subcellular fraction of human term placenta stored at -96 degrees C. *Endocr. Res.* **12**, 105–113.
- Toews A. D. and Morell P. (1981) Turnover of axonally transported phospholipids in nerve endings of retinal ganglion cells. *J. Neurochem.* **37**, 1316–1323.
- Truckenmiller M. E., Nambodiri M. A., Brownstein M. J. and Neale J. H. (1985) *N*-Acetylation of L-aspartate in the nervous system: differential distribution of a specific enzyme. *J. Neurochem.* **45**, 1658–1662.
- Tsai G. and Coyle J. T. (1995) *N*-Acetylaspartate in neuropsychiatric disorders. *Prog. Neurobiol.* **46**, 531–540.
- Urenjak J., Williams S. R., Gadian D. G. and Noble M. (1992) Specific expression of *N*-acetyl-aspartate in neurons, oligodendrocyte type-2 astrocyte progenitors, and immature oligodendrocytes in vitro. *J. Neurochem.* **59**, 55–61.